JOURNAL OF THERMOPHYSICS AND HEAT TRANSFER
Vol. 9, No. 4, October–December 1995

Experimental Support for the Lagging Behavior in Heat Propagation

Da Yu Tzou*
University of New Mexico, Albuquerque, New Mexico 87131

This work examines the lagging behavior for heat transport in small-scale and fast-transient processes. The experimental result by Qiu et al. for the femtosecond transient response in gold films and that by Bertman and Sandiford for the temperature pulse traveling through superfluid liquid helium are re-examined with emphasis on the lagging behavior. The model employing the phase-lag concept provides as competent or even better results when describing the special response observed in these experiments.

Nomenclature

A_i = coefficients in the Laplace transform solution, K s, $i = 1, 2, 3$
a = parameter in the normalized autocorrelation function, dimensionless
B = coefficient in the Laplace transform solution, 1/m
C = thermal wave speed, m/s
C_e, C_l = volumetric heat capacity of the electron gas and the metal lattice, J/m³ K
C_p = averaged volumetric heat capacity in the conducting medium, J/m³ K
C_1 = coefficient in the Laplace transform solution, m K/W
C_2 = coefficient in the Laplace transform solution, m K s/W
G = electron–phonon coupling factor, W/m³ K
h = step functions
I = power intensity of laser beam, W/m²
J = energy intensity of laser pulse, J/m²
K = thermal conductivity, W/m K
k = a parameter, equivalent to τ_T/τ_q
L = thickness of the thin film, μm
l = dimensionless thickness of the thin film
M, N = orders of the Taylor series expansion
p = Laplace transform parameter, 1/s
q = heat flux, W/m²
R = reflectivity, dimensionless
Re = real part of the function
R_τ = ratio of (τ_T/τ_q)
r = space variable, m
S = energy-absorption-rate, W/m³
T = absolute temperature, K
t = time, s
t_p = laser pulse duration, s
x = space variable, m
α = thermal diffusivity, m²/s
β = dimensionless time
δ = penetration depth of laser beam, m
ε = parameter in the normalized autocorrelation function, 1/s
η = dimensionless heat flux
θ = dimensionless temperature
ξ = dimensionless space
τ = relaxation time in the heat flux equation of the Jeffreys type, s
τ_R, τ_N = relaxation times in the umklapp and normal processes of phonon scattering, s
τ_T, τ_q = phase lags of the temperature gradient and the heat flux vector, s

Subscripts
b = quantity at boundaries
F = quantities calculated at the Fermi surface
max = maximum value
p = laser pulse
s = pulse quantities
0 = ambient conditions, constant

Superscripts
$\bar{}$ = Laplace transform
$*$ = equivalent properties

Introduction

HEAT propagation in solids, traditionally, has been interpreted as either a diffusion or a wave phenomenon. In the absence of a time-varying heat source and an oscillatory boundary excitation, the diffusion theory always results in a decayed temperature in time due to involvement of the first-order time-derivative in the diffusion equation. The thermal wave model, on the other hand, involves a wave term in the energy equation. It introduces a sharp wavefront in the history of thermal wave propagation, resulting in several physical phenomena that cannot be depicted by diffusion. They include the thermal shock formation around a fast-moving heat source[1–3] or a rapidly-propagating crack tip[4,5] and the thermal resonance phenomenon under frequency excitations.[6] Detailed reviews for research in the area of thermal waves can be found in the articles by Joseph and Preziosi,[7,8] Tzou,[9] and more recently, Özisik and Tzou.[10]

Although the thermal wave behavior has been recognized as a possibility for capturing the microscale response in time in some situations,[11] strictly speaking, there exists no direct experimental evidence so far that supports the classical thermal wave behavior proposed by Cattaneo[12] and Vernotte[13,14] (abbreviated by CV-wave in this work). A possible reason may be the lack of a consistent description for the simultaneous microscale response in space, evidenced by its limited applicability to only the optically thick medium.[15,16] The importance of such an effect can be well-illustrated by reviewing the femtosecond (fs) transient response in gold films obtained experimentally by Brorson et al.[17] The heat transport velocity in gold films, according to their experimental result, is on the order of 10^6 m/s. For a transient response occurred in pico-

Received Oct. 3, 1994; revision received Jan. 20, 1995; accepted for publication March 16, 1995.
*Associate Professor, Department of Mechanical Engineering. Member AIAA.

to femtoseconds, assuming a wave behavior, this implies a thermal penetration depth on the orders from micro- to nanometers. Heat transport in such a small scale comparable to the mean-free-path of phonon–electron collision, obviously, necessitates a simultaneous consideration of the microstructural interaction effects, including phonon scattering from grain boundaries and/or phonon–electron interactions, in the theoretical framework. Because the classical CV-wave model does not account for these microstructural effects, it is expected to fail when heat transport process is dominated by these microscopic mechanisms.

A parallel consideration can be given to heat conduction at low temperatures. For heat transport to take place, first of all, molecules inside the conducting medium need to be activated to a certain energy level. This is not a problem for heat conduction at room temperature because the room temperature is much higher than the activation energy of molecules for most media. For heat conduction in superfluid liquid helium at about 1 K, however, the delayed response due to the time required for establishing the activation energy of molecules in the liquid helium may induce a completely different behavior from what we have known. None of the existing models, including the conventional CV-wave model, reflects such a microscopic mechanism in its framework.

The present work revisits the experimental results obtained by Bertman and Sandiford[18] for a temperature pulse propagating in superfluid liquid helium and those by Brorson et al.,[17] Qiu and Tien,[19] and Qiu et al.[20] for femtosecond transient responses in gold film. While the inert behavior of molecules causes the lagging response for heat propagation in liquid helium, the delayed response in the ultrafast laser heating on gold films is attributed to the finite time required for the phonon–electron interaction to take place. The dual-phase-lag (DPL) model recently proposed by Tzou[17,18] for small-scale, fast-transient heat transport process will be used to explore the lagging behavior observed in these experiments. Although they are often cited as the evidences supporting the CV-wave behavior (for heat propagation in liquid helium) and the phonon–electron coupling in microscale (fast laser-heating on metals), this work shows that the dual-phase-lag model yields as competitive results when describing the special features observed in these experiments.

Lagging Behavior

The dual-phase-lag model[21,22] incorporates the microstructural interaction effect in the fast-transient process of heat transport. In short, it describes the finite time required for the various microstructural interactions to take place, including the phonon–electron interaction in metals, the phonon scattering in dielectric crystals, insulators, and semiconductors, and the activation of molecules at extremely low temperature, by the resulting phase-lag (time-delay) in the process of heat transport. When heat transport occurs at a general time t in the transient process, described by the energy equation

$$-\nabla\cdot\boldsymbol{q}(\boldsymbol{r}, t) = C_p \frac{\partial T(\boldsymbol{r}, t)}{\partial t} \tag{1}$$

the DPL distinguishes the time instant $t + \tau_q$, at which the heat flux flows through a material volume and the time instant $t + \tau_T$, at which the temperature gradient establishes across the same material volume:

$$\boldsymbol{q}(\boldsymbol{r}, t + \tau_q) = -K\nabla T(\boldsymbol{r}, t + \tau_T) \tag{2}$$

In addition to the thermal conductivity, the phase lags τ_T and τ_q are treated as two additional intrinsic thermal properties characterizing the energy-bearing capacity of the material. For the conducting media with $\tau_T > \tau_q$, the heat flux vector precedes the temperature gradient in the time-history, implying that the heat flux vector is the cause while the temperature gradient is the effect of the heat flow. For the media with $\tau_q > \tau_T$, on the other hand, the temperature gradient becomes the cause while the heat flux vector becomes the effect. Such an interchange between the cause and the effect in the transient process of heat flow cannot be depicted by the classical theory of diffusion where the response is assumed to be instantaneous.

Equations (1) and (2) describing the lagging behavior in heat transport display two coupled differential equations of a delayed type. Due to the general time shifts at different scales, τ_T and τ_q, no general solution has been known yet. The refined structure of the lagging response depicted by Eqs. (1) and (2), however, can be illustrated by expanding Eq. (2) in terms of the Taylor's series with respect to time:

$$\boldsymbol{q}(\boldsymbol{r}, t) + \sum_{i=1}^{N} \frac{\tau_q^{(i)}}{(i)!} \frac{\partial^{(i)}\boldsymbol{q}}{\partial t^{(i)}}(\boldsymbol{r}, t) = -K\left\{\nabla T(\boldsymbol{r}, t) + \sum_{j=1}^{M} \frac{\tau_T^{(j)}}{(j)!} \frac{\partial^{(j)}}{\partial t^{(j)}}[\nabla T(\boldsymbol{r}, t)]\right\}, \qquad M, N \geq 1 \tag{3}$$

For an exact representation of Eq. (2), the number of terms, M and N in Eq. (3), must approach infinity. All the physical quantities in Eq. (3) now occur at time t, facilitating a further combination with the energy equation (1). The result is, for $T \equiv T(\boldsymbol{r}, t)$

$$\nabla^2 T + \sum_{i=1}^{M} \frac{\tau_T^{(i)}}{(i)!} \frac{\partial^{(i)}}{\partial t^{(i)}}(\nabla^2 T) = \frac{1}{\alpha}\left[\frac{\partial T}{\partial t} + \sum_{j=1}^{N} \frac{\tau_q^{(j)}}{(j)!} \frac{\partial^{(j+1)} T}{\partial t^{(j+1)}}\right] \tag{4}$$

Equation (4) dictates a progressive interchange between the diffusive and wave behaviors. When $N = M$, implying equal terms are taken in the Taylor series expansion on both sides of Eq. (3), Eq. (4) can be rearranged into the following form:

$$\frac{1}{N!} \frac{\partial^{(M)}}{\partial t^{(M)}}\left[\tau_T^M \nabla^2 T - \frac{\tau_q^M}{\alpha} \frac{\partial T}{\partial t}\right] + \text{lower-order terms} = 0 \tag{5}$$

The quantities enclosed by the brackets dictate the characteristics of the solution because they possess the highest-order differentials. A particular solution of Eq. (5) is easily seen

$$\nabla^2 T - \frac{1}{\alpha^*} \frac{\partial T}{\partial t} = 0 \quad \text{with} \quad \alpha^* = \alpha\left(\frac{\tau_T}{\tau_q}\right)^M \tag{6}$$

which is a diffusion equation with an equivalent thermal diffusivity α^*. The diffusive behavior depicted by Eq. (3) in the case of $M = N$ is thus clear. For $N = M + 1$, the next term taken after $N = M$ in the series approximation, the corresponding equation to Eq. (5) reads

$$\frac{\partial^{(M)}}{\partial t^{(M)}}\left[\frac{\tau_T^M}{M!} \nabla^2 T - \frac{1}{\alpha} \frac{\tau_q^{(M+1)}}{(M+1)!} \frac{\partial^2 T}{\partial t^2}\right] + \text{low-order terms} = 0 \tag{7}$$

It renders a wave equation as the particular solution:

$$\nabla^2 T - \frac{1}{C^{*2}} \frac{\partial^2 T}{\partial t^2} = 0 \quad \text{with} \quad C^* = \sqrt{\frac{(M+1)\alpha\tau_T^M}{\tau_q^{(M+1)}}} = C\sqrt{(M+1)\left(\frac{\tau_T}{\tau_q}\right)^M} \tag{8}$$

where $C = \sqrt{\alpha/\tau_q}$ is the speed of CV-waves.[23] Equation (8) demonstrates the subsequent wave behavior ($N = M + 1$) after diffusion [$N = M$, Eq. (6)]. When the subsequent modes

of high-order waves in Eq. (4) are gradually taken into account, the wave speed may become either slower or faster, depending on the ratio of (τ_T/τ_q). In passing, note that Eqs. (5–8) are only valid for nonzero values of τ_T and τ_q. For $\tau_T = 0$ or $\tau_q = 0$, the resulting energy equation should be found from Eq. (4).

It is now clear that the general lagging behavior represented by Eq. (2) is a combination of a series of diffusion and the wave behavior represented by Eq. (8). Before a general solution is obtained, however, it is the author's belief that finding the correlation to the well-developed microscopic and macroscopic models, though in the limiting cases, and searching for the possible experimental supports are more important than the full expansions into the nonlinear regimes of τ_T and τ_q. Bearing this in mind, the DPL has captured six representative models by its first- and second-order expansions.[21,22]

(a) Macroscopic diffusion model: The classical theory of diffusion is retrieved when $\tau_T = \tau_q$ in Eq. (6), including the case of $\tau_T = \tau_q = 0$ in Eq. (4). Equation (2) involves a trivial shift in the time-scale and reduces to the Fourier law assuming an instantaneous response between the heat flux vector and the temperature gradient.

(b) Macroscopic CV-wave model: $\tau_T = 0$, $N = 1$, and $\tau_q = \tau = \alpha/C^2$. Equation (4) reduces to the classical CV-wave equation, with C being the finite speed of heat propagation. It describes a wave behavior in the short-time response (a microscale response in time[10,11]), but its applicability is limited to the acoustically-thick media (a macroscale response in space[15,16]). Through the correlation of $\tau_q = \tau$, it is clear that the phase-lag τ_q describes the relaxation time due to the fast-transient effect of thermal inertia. Since $\tau_T = 0$ and $\tau_q = \tau > 0$ $(\tau_q > \tau_T)$, most importantly, the CV-wave model presumes precedence of the temperature gradient (cause) to the heat flux vector (effect) in the time-history. Such a strong assumption may be one of the reasons for limiting the extension of the CV-wave model to the microscale heat transfer in space.

The first-order approximation, $M = N = 1$ in Eq. (4), results in

$$\nabla^2 T(\boldsymbol{r}, t) + \tau_T \frac{\partial}{\partial t} \nabla^2 T(\boldsymbol{r}, t) = \frac{1}{\alpha} \frac{\partial T}{\partial t} + \frac{\tau_q}{\alpha} \frac{\partial^2 T}{\partial t^2} \tag{9}$$

Though containing a wave term, as described by Eq. (6), Eq. (9) remains diffusive (parabolic)[7,8] and does not possess a sharp wavefront due to the strong effect of dispersion from τ_T.[21,22] Equation (9) describes the following.

(c) Phenomenological heat flux equation of the Jeffreys type: Joseph and Preziosi[7,8] provided a detailed discussion of the Jeffreys-type heat flux equation based on the concept of effective thermal conductivity. It appears as a special case of Eq. (9), with $\tau_T \equiv k_1 \tau$ and $\tau_q \equiv \tau$. The parameter k_1 in the heat flux equation of the Jeffreys type, obviously, corresponds to the ratio of (τ_T/τ_q) in the DPL.

(d) Microscopic two-step model (parabolic type): The microscopic two-step model[24–27] describes the effect of phonon–electron interaction for microscale heat transport in metals. Along with the volumetric heat capacities of the electron gas C_e and the metal-lattice C_l, the phonon–electron coupling factor G dominates the short-time energy transport between electrons and phonons. Tzou[21,22] showed that the single energy equations governing the electron-gas temperature and the metal-lattice temperature have the same form. Both are identical to that shown by Eq. (9), with the following correspondence:

$$\begin{aligned} \alpha &= K/(C_e + C_l), \qquad \tau_t = C_l/G \\ \tau_q &= (1/G)[(1/C_e) + (1/C_l)]^{-1} \end{aligned} \tag{10}$$

G is a dominating microscopic property (microscale effect in space) that causes the time delays (τ_T and τ_q, microscale effect in time) for heat transport on a macroscopic level. Note that the correspondence shown by Eq. (10) assumes constant thermal properties. According to experimental data for G,[17,26] the values of τ_T and τ_q are, respectively, 70.833 and 0.4648 ps for Cu, 89.286 and 0.7438 ps for both Au and Ag, and 12.097 and 0.172 ps for Pb.[21] When the temperature-dependent properties, such as heat capacity of the electron gas, are taken into account, the perfect correlation shown by Eq. (10) still exists, but the equivalent heat capacity in the DPL is governed by a nonlinear partial differential equation.

(e) Microscopic phonon-scattering model: The pure-phonon scattering model proposed by Guyer and Krumhansl[7,28] applies to the microscale heat transport in dielectric films, insulators, and semiconductors. Although its constitutive equation does not reduce to the Fourier law in steady state, the combined energy equation results in an identical form to Eq. (9).[7,21] In correlation to the microscopic properties, it yields

$$\alpha = \tau_R c^2/3, \qquad \tau_T = 9\tau_N/5, \qquad \tau_q = \tau_R \tag{11}$$

While the phase-lag of the temperature gradient τ_T stretches the relaxation time in the normal process of phonon collision τ_N by a constant factor of 9/5, the phase-lag of the heat flux vector, τ_q is equivalent to the relaxation time in the umklapp process describing the momentum loss in phonon collision τ_R.

(f) Microscopic two-step model (hyperbolic): The second-order effect of τ_q, $M = 1$ and $N = 2$ in Eq. (4), results in

$$\nabla^2 T(\boldsymbol{r}, t) + \tau_T \frac{\partial}{\partial t} \nabla^2 T(\boldsymbol{r}, t) = \frac{1}{\alpha} \frac{\partial T}{\partial t} + \frac{\tau_q}{\alpha} \frac{\partial^2 T}{\partial t^2} + \frac{\tau_q^2}{2\alpha} \frac{\partial^3 T}{\partial t^3} \tag{12}$$

This equation has exactly the same form as the energy equation in the hyperbolic two-step model accounting for the ballistic behavior of heat transport in the electron gas.[19,20,27] The correspondence to the DPL results

$$\alpha = \frac{K}{C_e + C_l}, \qquad \tau_T = \frac{C_l}{G}, \qquad \tau_q = \tau_F + \frac{1}{G}\left(\frac{1}{C_e} + \frac{1}{C_l}\right)^{-1} \tag{13}$$

in this case, with the relaxation time of the electron-gas at the Fermi surface τ_F appearing as an added effect to τ_q. Equation (12) depicts a wave behavior in the history of heat propagation. The wave speed is represented by Eq. (8) with $M = 1$.

Qiu and Tien[19] characterized the parabolic (the diffusion model in a) and hyperbolic (the CV-wave model in b) one-step models, and the parabolic d and hyperbolic e two-step models by comparing the heating time to the thermalization time and the relaxation time in the transient process. The hyperbolic two-step model reduces to the parabolic two-step model as the heating time is much greater than the relaxation time. Within the context of the DPL, refer to Eq. (12) containing the τ_q^2 effect, this is equivalent to the condition of $(t/\tau_q)^2 \to 0$. The resulting equation containing the first-order effects of (t/τ_q) and (t/τ_T) reduces to the parabolic two-step equation, Eq. (9). The correspondence of τ_q to the relaxation time is thus evident. The relaxation behavior results in a wave phenomenon in heat propagation.[27] The parabolic two-step model further reduces to the parabolic one-step model should the heating time be much greater than the thermalization time. In view of Eq. (9), this imposes an additional condition of $(t/\tau_T) \to 0$, implying the correspondence of τ_T to the thermalization time. The thermalization time characterizes the time period for phonons and electrons to achieve thermodynamic equilibrium. Unlike the relaxation behavior, the thermalization process does not induce a wave behavior in heat propagation.[27]

The precise physical meanings of τ_T and τ_q need to be determined by the microscopic approach employing the Boltzmann transport equation. This important task is currently

under way. Before an explicit result is obtained, however, the correlations to the various models express the two phase-lags in terms of the macroscopic and microscopic parameters that have been fully explored. Since many of these models have been shown admissible within the semiclassical framework (such as the hyperbolic two-step model[27]), the precise correlations shown from a to f may be viewed as an indirect support of the DPL at this stage of development.

Lagging Behavior Due to Phonon–Electron Interaction

Brorson et al.[17] and Qiu et al.[20] performed novel experiments of the femtosecond laser-heating on gold films. In brief, the sample was heated by an intense beam (pump beam), whereas the reflectivity change at sample surfaces was measured by a weak beam (probe beam). The time delays between the pump and the probe beams were controlled by a mirror mounted on a variable optical delay stage. Placing the mirror at different positions causes a change in the optical path between the pump and probe beams, which in turn results in various time delays between the two pulses. A detailed illustration for the experimental system is provided by Qiu et al.,[20] which will not be repeated here. The major mechanisms under study include the fast-transient phonon–electron interaction and the excessively high temperature established in the electron gas in extremely short times.

Inspired by the correspondence shown in Eq. (10), which supports the basis of viewing the microstructural interaction effect (in space, through G) by its resulting delayed response in time (through τ_T and τ_q), the possible lagging behavior in these experiments is examined by incorporating the simplest case containing the first-order effect of τ_T and τ_q [$M = N = 1$, Eq. (9)].

The gold film is modeled by a one-dimensional solid, with the laser-heating described by the energy-absorption rate.[19,20,26,27] In the presence of a body heating $S(x, t)$, Eq. (9) becomes[21,22]

$$\frac{\partial^2 T}{\partial x^2} + \tau_T \frac{\partial^3 T}{\partial x^2 \partial t} + \frac{1}{K}\left(S + \tau_q \frac{\partial S}{\partial t}\right) = \frac{1}{\alpha}\frac{\partial T}{\partial t} + \frac{\tau_q}{\alpha}\frac{\partial^2 T}{\partial t^2} \tag{14}$$

The time-derivative of S is the apparent heat source term resulting from the fast-transient effect of thermal inertia described by τ_q.[21,22] Determination of the energy-absorption rate itself is a complex task, involving the estimate of the full-width-at-half-maximum pulse duration t_p and the approximation of the pulse shape by a Gaussian distribution. All of the parameters from Qiu and Tien[20] are adopted except a slight modification of the Gaussian profile to better-fit the experimental curve of the normalized autocorrelation function:

$$\frac{I_s(t)}{I_s(0)} = \begin{cases} e^{-\varepsilon t} + \varepsilon t e^{-\varepsilon t}, & t \geq 0 \\ e^{\varepsilon t} - \varepsilon t e^{\varepsilon t}, & t \leq 0 \end{cases} \quad \text{with} \quad \varepsilon = \frac{a}{t_p} \tag{15}$$

For $t_p = 100$ fs, comparison of Eq. (15) with the experimental result is shown in Fig. 1. The resulting energy-absorption rate is

$$S(x, t) = S_0 \exp\{-(x/\delta) - [a|(t - 2t_p)|/t_p]\}$$

with

$$S_0 = 0.94[(1 - R)/t_p\delta]J \tag{16}$$

Within the context of the first-order approximation, Eqs. (14) and (16) describe the process of heat transport with a lagging behavior. The physical mechanisms for the lagging response, to be reiterated, are the fast-transient effect of thermal inertia

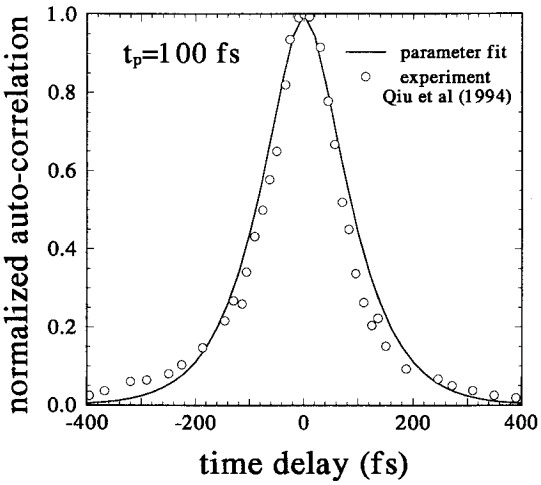

Fig. 1 Normalized autocorrelation function for the power intensity of laser beam [Eq. (15)], and comparison with the experimental result.[20] t_p = 100 fs, a = 1.88.

τ_q in short-time response and the finite time required for the phonon–electron interaction in microscale to take place, τ_T.

The gold film is assumed to be heated from a stationary state, implying that

$$T(x, 0) = T_0 \quad \text{and} \quad \frac{\partial T}{\partial t}(x, 0) = 0 \tag{17}$$

The film-thickness is assumed to be a constant L. During the short period of laser heating, heat losses from the front and back surfaces are assumed negligible,[20] implying that

$$\frac{\partial T}{\partial x}(0, t) = \frac{\partial T}{\partial x}(L, t) = 0 \tag{18}$$

The solution of Eq. (14) subjected to the initial and boundary conditions (17) and (18) can be obtained by the method of Laplace transform employing the Riemann-sum approximation[29,30] for the Laplace inversion. The result is

$$T(x, t) = T_0 + \frac{e^{4.7}}{t}\left\{\frac{\bar{T}[x, (4.7/t)]}{2} + \text{Re}\sum_{n=1}^{N}(-1)^n \bar{T}\left(x, \frac{4.7 + in\pi}{t}\right)\right\} \tag{19}$$

where the constant 4.7 results from the optimal value ensuring a fast numerical convergence, and $\bar{T}(x, p)$ is the Laplace transform solution satisfying Eqs. (14) and (16–18):

$$\bar{T}(x, p) = A_1 e^{Bx} + A_2 e^{-Bx} + A_3 e^{-x/\delta} \tag{20}$$

$$A_1 = \frac{(A_3/\delta)(e^{-L/\delta} - e^{-BL})}{B(e^{BL} - e^{-BL})}, \qquad A_2 = A_1 - \frac{A_3}{B\delta} \tag{20a}$$

$$A_3 = \frac{S_0(C_2 e^{-2a} - C_1 S_b)}{(1/\delta)^2 - B^2}, \qquad B = \sqrt{\frac{p(1 + p\tau_q)}{\alpha(1 + p\tau_T)}}$$

$$C_1 = \frac{1 + p\tau_q}{K(1 + p\tau_T)}, \qquad C_2 = \frac{\tau_q}{K(1 + p\tau_T)} \tag{20b}$$

$$S_b = t_p\left(\frac{e^{-2a} - e^{-2pt_p}}{pt_p - a} + \frac{e^{-2pt_p}}{pt_p + a}\right)$$

Equation (19) is used to calculate the normalized temperature change, $\Delta T(0, t)/[\Delta T((0, t)]_{\max}$, at the front surface of the gold film at $x = 0$. This quantity, after a few hundred fem-

toseconds of the initial laser heating, is related to the measured reflectivity change.[20] These data are available for gold films with a thickness of 0.1 μm[17,20] and 0.2 μm,[17] respectively. In determining the appropriate values of τ_T and τ_q to describe the experimental curve, the inverse analysis[31] on the analytical basis shown by Eq. (10) is employed. The values estimated on the basis of constant thermal properties, $\tau_T = 89.286$ ps and $\tau_q = 0.7438$ ps for gold, however, are expected to change due to the strong temperature-dependent heat capacity of the electron-gas reflected in the experimental data. For $\tau_T = 90$ ps and $\tau_q = 8.5$ ps, the calculated reflectivity-change is shown in Fig. 2 along with the experimental results.[17,20] The agreement supports the lagging behavior proposed in this work. Compared to the values of τ_T and τ_q calculated under constant thermal properties, the value of τ_q (describing the fast-transient effect of thermal inertia) increases by approximately an order of magnitude, implying that τ_q is more sensitive to the temperature dependency of the thermal property than τ_T. The greater value of τ_T than τ_q ($\tau_T > \tau_q$) also implies that the heat flux vector (cause) precedes the temperature gradient (effect) in the ultrafast heating process. This may explain why the

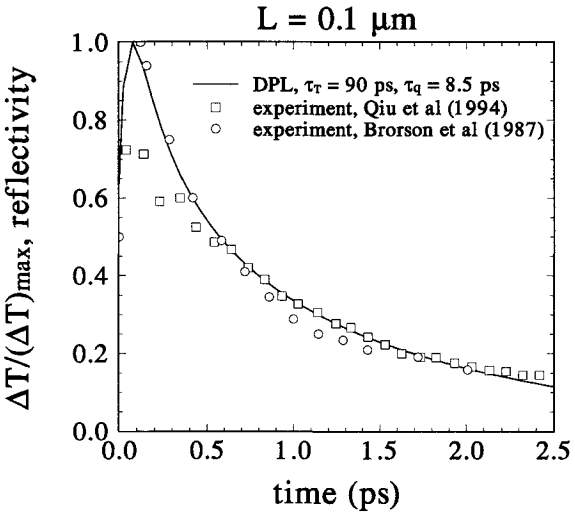

Fig. 2 Normalized temperature-change (reflectivity) in the femtosecond laser heating on gold films. Prediction of the DPL at the front surface ($x = 0$) and comparison with the experimental results.[17,20] $L = 0.1$ μm, $J = 13.4$ J/m^2, $R = 0.93$, $\delta = 15.3$ nm, $t_p = 100$ fs, $a = 1.88$, $\tau_T = 90$ ps, and $\tau_q = 8.5$ ps.

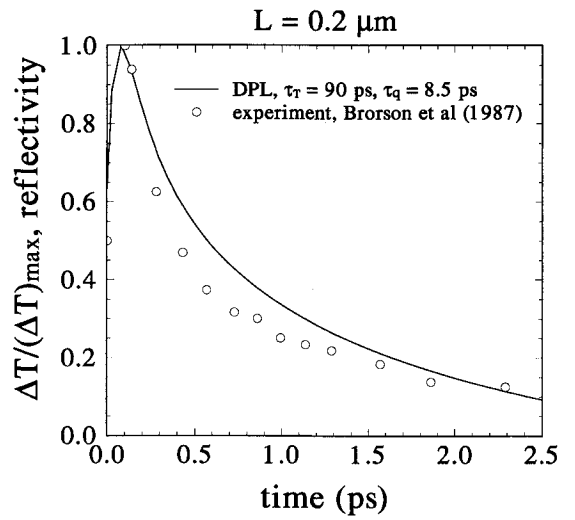

Fig. 3 Normalized temperature-change (reflectivity) at the front surface predicted by the DPL and comparison with the experimental result[17] in a thicker gold film, $L = 0.2$ μm.

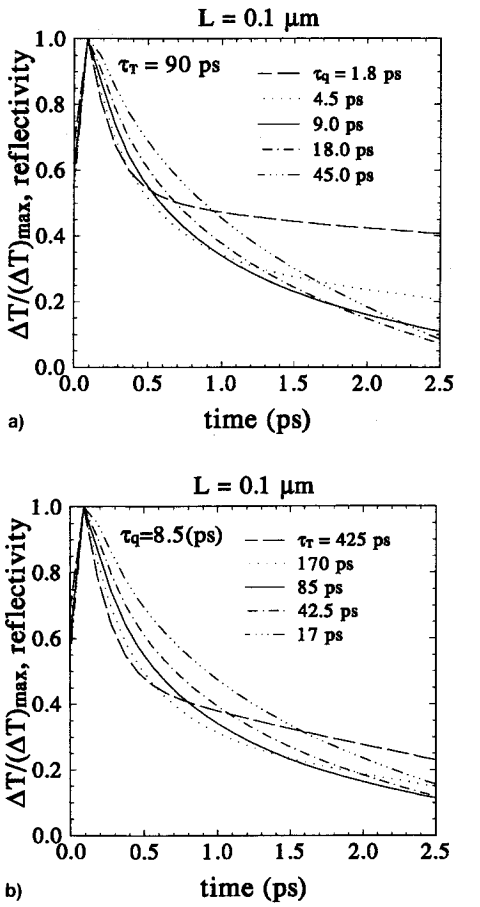

Fig. 4 Effects of a) τ_q and b) τ_T on the lagging behavior of the normalized temperature-change (reflectivity) at the front surface.

classical CV-wave model assuming a reversed relation, $\tau_q > \tau_T (=0)$, fails when used for describing the fast-transient phenomena in these experiments.[19,20,26,27] The results for the reflectivity-change in a thicker film, $L = 0.2$ μm, are shown in Fig. 3 under the same values of τ_T and τ_q. The satisfactory agreement supports that the two phase lags are indeed intrinsic thermal properties that do not vary with the sample size for $L \geq 0.1$ μm. Should the thickness be significantly reduced so that the microstructural configuration in the gold film (and, hence, the cumulated delayed times measuring the microstructural interaction effect through the thickness) be altered, however, the values of τ_T and τ_q (including their precedence-sequence) may dramatically change with the thickness. In performing the fast-transient experiment in the medium blasting sand,[32] the phase lags have been found very sensitive to the microstructures reflecting the rapid energy-change between the solid (sand particles) and the gaseous (pores) phases. Effects of τ_q and τ_T are illustrated in Figs. 4a and 4b, respectively. At a fixed value of τ_T (Fig. 4a), increasing the value of τ_q promotes (demotes) the temperature level at earlier (later) times. At a fixed value of τ_q (Fig. 4b), decreasing the value of τ_T produces the same effect. Bearing in mind that the classical theory of diffusion assumes an instantaneous response, i.e., $\tau_T = \tau_q = 0$, these are useful trends for the understanding of the fast-transient effect τ_q and the microstructural interaction effect τ_T.

Temperature Pulses in Liquid Helium

Bertman and Sandifords' experiment[18] gives the first result for the time-history of the temperature at a particular (fixed) position inside superfluid liquid helium at 4 K. They produced an electric pulse from a generator, which applies a thermal pulse to the liquid-helium sample and simultaneously triggers

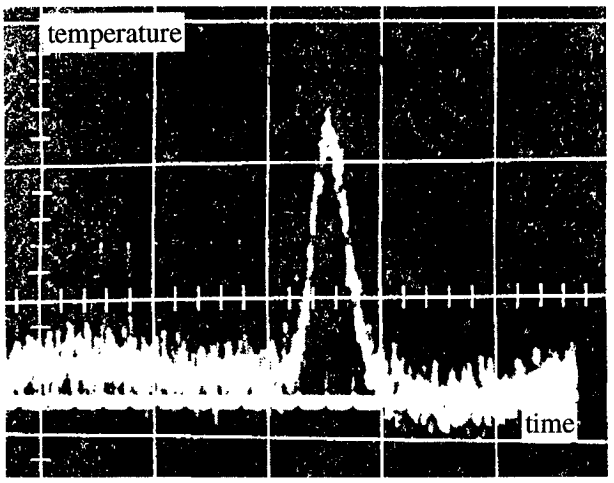

a)

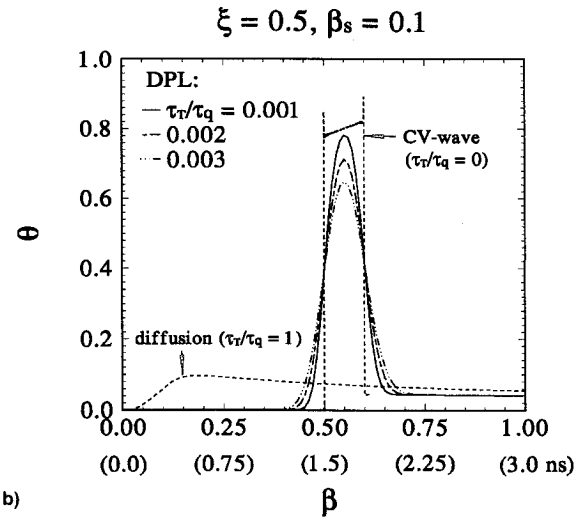

b)

Fig. 5 Temperature pulse propagating in superfluid liquid helium: a) the oscilloscope trace recorded experimentally[18] and b) the effect of τ_T on smoothening and spreading of the pulse shape.

the oscilloscope. The local temperature at the fixed position is recorded by a resistance-type of thermometer. A typical oscilloscope trace is shown in Fig. 5a. The rapid rise-and-fall behavior occurs after a certain time that the heat-pulse is applied to the end of the sample, implying that the temperature pulse propagates at a finite speed. When changing the probed position, only the time of arrival of the heat pulse changes, which is a characteristic of "thermal waves."

Due to the introductory nature, the temperature and time scales in Fig. 5a are not provided in the original paper. To describe the possible lagging behavior, which is attributed to the finite time required for establishing the activating energy of molecules for transporting heat through the liquid helium in this case, the experiment is simulated by a one-dimensional problem with an infinite extent (to remove the effect of reflection from the boundary). The energy equation describing the first-order effect of τ_T and τ_q is represented by Eq. (9). While the initial conditions remain the same [Eq. (17)], the thermal pulse is modeled by step functions with a finite duration t_s

$$q(0, t) = q_s[h(t) - h(t - t_s)], \qquad t_s \geq 0 \tag{21}$$

The temperature at infinity is assumed undisturbed, i.e., $T \to T_0$ as $x \to \infty$. A dimensionless analysis is more suitable for a qualitative description in the absence of the physical scales. Introducing

$$\eta = \frac{q}{q_s}, \qquad \theta = \frac{T - T_0}{q_s\sqrt{\alpha\tau_q}/K}, \qquad \beta_s = \frac{t_s}{\tau_q}$$
$$\beta = \frac{t}{\tau_q}, \qquad \xi = \frac{x}{\sqrt{\alpha\tau_q}} \tag{22}$$

Eq. (9) satisfying the initial condition (17) and the boundary condition (21) can be obtained in the same manner. The expression for temperature is given by Eq. (19), with T replaced by θ, x by ξ, and t by β, while the transformed solution becomes

$$\bar{\theta}(\xi, p) = \bar{\eta}_b(p)\sqrt{\frac{1 + p}{p[1 + p(\tau_T/\tau_q)]}}\exp\left[-\sqrt{\frac{p(1 + p)}{1 + p(\tau_T/\tau_q)}}\,\xi\right]$$

with

$$\bar{\eta}_b(p) = \frac{1 - e^{-\beta_s p}}{p} \tag{23}$$

Note that the solutions for diffusion ($\tau_T/\tau_q = 1$) and CV-wave ($\tau_T = 0$) are absorbed in Eq. (23). Along with these two special cases, the results for $(\tau_T/\tau_q) = 0.001$, 0.002, and 0.003 are shown in Fig. 5b for $\xi = 0.5$ and $\beta_s = 0.1$. Based on the threshold values of the thermal wave speed[33] and the thermal diffusivity[34] for liquid helium, $C = 19$ m/s and $\alpha = 1.083 \times 10^{-6}$ m^2/s, the estimated real times are enclosed in parentheses for reference. The classical theory of diffusion predicts an early rise of temperature that gradually decays in the time-

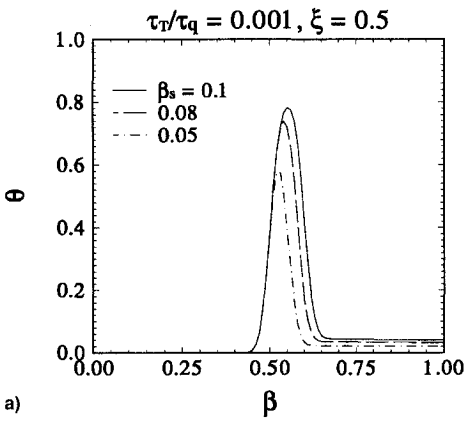

a)

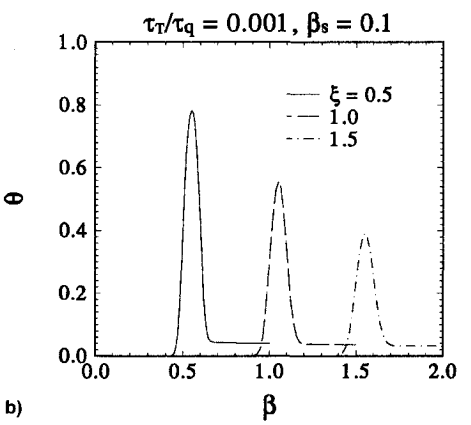

b)

Fig. 6 Temperature pulse propagating in superfluid liquid helium: a) the effect of pulse-width (β_s), $\tau_T/\tau_q = 0.001$ and $\xi = 0.5$ and b) the evolution of pulse shapes downstream, $\tau_T/\tau_q = 0.001$ and $\beta_s = 0.1$.

history. It does not describe the rapid rise-and-fall behavior observed in the oscilloscope trace in Fig. 5a. The CV-wave model, on the other hand, results in sharp edges in the temperature pulse on arrival and departure of the sharp wavefront. It closely resembles the pulse shape specified at the boundary. When the microstructural interaction effect activates, reflected by the gradually increasing value of τ_T describing the finite time required for activating the low-temperature molecules, the sharp edges of the temperature pulse become smoother and the peak value of temperature decreases. Outward-spreading of the temperature pulse renders a bell-shape that bears great resemblance to the oscilloscope trace recorded in the experiment, Fig. 5a. While Bertman and Sandifords' result is often referred to as an experimental evidence for the CV-wave behavior,[35] it seems that the DPL provides even more refined details for the rapid rise-and-fall response.

The rapid rise-and-fall behavior remains when shortening the pulse-width, as shown by Fig. 6a. The peak temperature decreases with the pulse-width β_s and the temperature pulse becomes more localized at smaller values of β_s. When propagating downstream, as shown by Fig. 6b, the peak temperature decreases, revealing the dispersive behavior in the lagging response. The response time for a significant temperature-change is prolonged downstream due to the fast-transient effect (the wave-like behavior) described by τ_q.

Conclusions

This work examines the possible lagging behavior in several well-known experiments. The experiments by Brorson et al.[17] and Qiu et al.[20] investigate the phonon–electron dynamics in the short-time transient in gold films. Absorbing the time-delay due to the fast-transient effect of thermal inertia in the phase-lag of the heat flux vector τ_q and the time-delay due to the finite time required for the phonon–electron interaction to take place in the phase-lag of the temperature gradient τ_T, evidenced by the agreements shown in Figs. 2 and 3, the DPL yields as competent predictions as the microscopic two-step model.[20,26,27] Equation (10) provides the physical basis for describing the microscale effect (phonon–electron interaction) in space in terms of the resulting delayed response in time. The agreements shown in Figs. 2 and 3 also suggest that the heat flux vector precedes the temperature gradient, i.e., $\tau_q < \tau_T$, when the lagging behavior is caused by the phonon–electron interaction. The lagging behavior for heat transport in superfluid liquid helium, in the second attempt, is attributed to the finite time required for activating the molecules at extremely low temperature. As shown in Fig. 5b, the time-delay τ_T smoothens the sharp edges resulting from the fast-transient effect, rendering a rapid rise-and-fall behavior that more closely resembles the oscilloscope trace shown in Fig. 5a. The temperature gradient, however, precedes the heat flux vector ($\tau_T < \tau_q$) in this case. The lagging behavior may be caused by different physical mechanisms. According to the two examples studied in this work, the preceding quantity in heat flow seems to sensitively vary with the substructural mechanisms causing delays. Including the possible consequences, this is an interesting feature to be further analyzed by the Boltzmann transport equation.

Both the microscopic two-step model and the DPL make an attempt to use temperature, a well-defined quantity only for equilibrium processes, in describing the nonequilibrium thermodynamic transition that occurred in extremely short times. Convenience and familiarity to the treatment are obviously two major purposes, but their suitability (in the sense of engineering approximations) has been well-justified by the agreement to the experimental results.[20,26,27] The two-step model captures the nonequilibrium feature in transition of the thermodynamic states by the continual energy-exchange between phonons and electrons throughout the transient process. In the context of DPL, alternately, the nonequilibrium feature is reflected by the inequality between $-K\nabla T$ and $\boldsymbol{q}$ at the same instant of time, i.e., $\boldsymbol{q}(t) \neq -K\nabla T(t)$. The difference between the two [refer to Eq. (2)], depends on the values of τ_T and τ_q, which may be viewed as a measure for the degree of nonequilibrium between the temperature gradient and the heat flux vector in the transient process.

References

[1]Tzou, D. Y., "On the Thermal Shock Wave Induced by a Moving Heat Source," *Journal of Heat Transfer*, Vol. 111, No. 2, 1989, pp. 232–238.

[2]Tzou, D. Y., "Shock Wave Formation Around a Moving Heat Source in a Solid with Finite Speed of Heat Propagation," *International Journal of Heat and Mass Transfer*, Vol. 32, No. 10, 1989, pp. 1979–1987.

[3]Tzou, D. Y., "Three Dimensional Structures of the Thermal Shock Waves Around a Rapidly Moving Heat Source," *International Journal of Engineering Science*, Vol. 28, No. 10, 1990, pp. 1003–1017.

[4]Tzou, D. Y., "Thermal Shock Waves Induced by a Moving Crack," *Journal of Heat Transfer*, Vol. 12, No. 1, 1990, pp. 21–27.

[5]Tzou, D. Y., "Thermal Shock Wave Induced by a Moving Crack—A Heat Flux Formulation," *International Journal of Heat and Mass Transfer*, Vol. 33, No. 4, 1990, pp. 877–885.

[6]Tzou, D. Y., "Thermal Resonance Under Frequency Excitations," *Journal of Heat Transfer*, Vol. 114, No. 2, 1992, pp. 310–316.

[7]Joseph, D. D., and Preziosi, L., "Heat Waves," *Reviews of Modern Physics*, Vol. 61, No. 1, 1989, pp. 41–73.

[8]Joseph, D. D., and Preziosi, L., "Addendum to the Paper on Heat Waves," *Review of Modern Physics*, Vol. 62, No. 2, 1990, pp. 375–391.

[9]Tzou, D. Y., "The Thermal Shock Phenomena in Solids Under High-Rate Response," *Annual Review of Heat Transfer*, edited by Chang-Lin Tien, Vol. IV, Hemisphere, Washington, DC, 1992, pp. 111–185, Chap. 3.

[10]Özisik, M. N., and Tzou, D. Y., "On the Wave Theory in Heat Conduction," *Journal of Heat Transfer*, Vol. 116, No. 3, 1994, pp. 526–535.

[11]Goodson, K. E., and Flik, M. I., "Microscale Phonon Transport in Dielectrics and Intrinsic Semiconductors," *Fundamental Issues in Small Scale Heat Transfer*, edited by Y. Bayazitoglu and G. P. Peterson, American Society of Mechanical Engineers HTD-Vol. 227, 1992, pp. 29–36.

[12]Cattaneo, C., "A Form of Heat Conduction Equation Which Eliminates the Paradox of Instantaneous Propagation," *Compte Rendus*, Vol. 247, No. 2, 1958, pp. 431–433.

[13]Vernotte, P., "Les Paradoxes de la Théorie Continue de L'équation de la Chaleur," *Compte Rendus*, Vol. 246, 1958, pp. 3154, 3155.

[14]Vernotte, P., "Some Possible Complications in the Phenomena of Thermal Conduction," *Compte Rendus*, Vol. 252, No. 12, 1961, pp. 2190, 2191.

[15]Majumdar, A., "Microscale Heat Conduction in Dielectric Thin Films," *Journal of Heat Transfer*, Vol. 115, No. 1, 1993, pp. 7–16.

[16]Joshi, A. A., and Majumdar, A., "Transient Ballistic and Diffusive Phonon Heat Transport in Thin Films," *Journal of Applied Physics*, Vol. 74, No. 1, 1993, pp. 31–39.

[17]Brorson, S. D., Fujimoto, J. G., and Ippen, E. P., "Femtosecond Electron Heat-Transport Dynamics in Thin Gold Film," *Physical Review Letters*, Vol. 59, No. 17, 1987, pp. 1962–1965.

[18]Bertman, B., and Sandiford, D. J., "Second Sound in Solid Helium," *Scientific America*, Vol. 222, No. 6, 1970, pp. 92–101.

[19]Qiu, T. Q., and Tien, C. L., "Femtosecond Laser Heating of Multi-Layered Metals—I. Analysis," *International Journal of Heat and Mass Transfer*, Vol. 37, No. 17, 1994, pp. 2789–2797.

[20]Qiu, T. Q., Juhasz, T., Suarez, C., Bron, W. E., and Tien, C. L., "Femtosecond Laser Heating of Multi-Layered Metals—II. Experiments," *International Journal of Heat and Mass Transfer*, Vol. 37, No. 17, 1994, pp. 2799–2808.

[21]Tzou, D. Y., "A Unified Field Approach for Heat Conduction from Micro- to Macro-Scales," *Journal of Heat Transfer*, Vol. 117, No. 1, 1995, pp. 8–16.

[22]Tzou, D. Y., "The Generalized Lagging Response in Small-Scale and High-Rate Heating," *International Journal of Heat and Mass Transfer* (to be published).

[23]Chester, M., "Second Sound in Solids," *Physical Review*, Vol. 131, No. 7, 1963, pp. 2013–2015.

[24]Kaganov, M. I., Lifshitz, I. M., and Tanatarov, M. V., "Relax-

ation Between Electrons and Crystalline Lattices," *Soviet Physics—JETP*, Vol. 4, No. 1, 1957, pp. 173–178.

[25]Anisimov, S. I., Kapeliovich, B. L., and Perel'man, T. L., "Electron Emission from Metal Surfaces Exposed to Ultra-Short Laser Pulses," *Soviet Physics—JETP*, Vol. 39, No. 2, 1974, pp. 375–377.

[26]Qiu, T. Q., and Tien, C. L., "Short-Pulse Laser Heating on Metals," *International Journal of Heat and Mass Transfer*, Vol. 35, No. 3, 1992, pp. 719–726.

[27]Qiu, T. Q., and Tien, C. L., "Heat Transfer Mechanisms During Short-Pulse Laser Heating of Metals," *Journal of Heat Transfer*, Vol. 115, No. 4, 1993, pp. 835–841.

[28]Guyer, R. A., and Krumhansl, J. A., "Solution of the Linearized Boltzmann Equation," *Physical Review*, Vol. 148, No. 3, 1966, pp. 766–778.

[29]Tzou, D. Y., Özisik, M. N., and Chiffelle, R. J., "The Lattice Temperature in the Microscopic Two-Step Model," *Journal of Heat Transfer*, Vol. 116, No. 4, 1994, pp. 1034–1038.

[30]Chiffelle, R. J., "On the Wave Behavior and Rate Effect of Thermal and Thermomechanical Waves," M.S. Thesis, Univ. of New Mexico, Albuquerque, NM, 1994.

[31]Orlande, H. R. B., Özisik, M. N., and Tzou, D. Y., "Inverse Analysis for Estimating the Electron-Phonon Coupling Factor in Thin Metal Films," *International Journal of Heat and Mass Transfer* (to be published).

[32]Tzou, D. Y., Leith, J. R., Xu, Y.-S., Guo, Y.-K. and Guo, Z.-Y., "The Nonhomogeneous Lagging Behavior in Porous Media," *International Journal of Heat and Mass Transfer* (to be published).

[33]Peshkov, V., "Second Sound in Helium II," *Journal of Physics* (U.S.S.R), Vol. 8, No. 4, 1944, pp. 381–385.

[34]Eckert, E. R. G., and Drake, R. M., Jr., *Analysis of Heat and Mass Transfer*, McGraw–Hill, New York, 1972, p. 780.

[35]Vick, B., and Özisik, M. N., "Growth and Decay of a Thermal Pulse Predicted by the Hyperbolic Heat Conduction Equation," *Journal of Heat Transfer*, Vol. 105, No. 4, 1983, pp. 902–907.